International Journal for Parasitology: Drugs and Drug Resistance 7 (2017) 147–158

Contents lists available at ScienceDirect

International Journal for Parasitology: Drugs and Drug Resistance

journal homepage: www.elsevier.com/locate/ijpddr

Proteomic and functional analyses reveal pleiotropic action of the anti-tumoral compound NBDHEX in *Giardia duodenalis*

Serena Camerini [a], Alessio Bocedi [b], Serena Cecchetti [a], Marialuisa Casella [a], Miriam Carbo [c], Veronica Morea [c], Edoardo Pozio [d], Giorgio Ricci [b, **], Marco Lalle [d, *]

[a] Department of Cell Biology and Neurosciences, Istituto Superiore di Sanità, viale Regina Elena 299, 00161 Rome, Italy
[b] Department of Chemical Sciences and Technologies, University of Rome "Tor Vergata", via della Ricerca Scientifica 1, 00133 Rome, Italy
[c] Institute of Molecular Biology and Pathology, CNR - National Research Council of Italy, Department of Biochemical Sciences "A. Rossi-Fanelli", "Sapienza" University, 00185 Rome, Italy
[d] Department of Infectious Diseases, Istituto Superiore di Sanità, viale Regina Elena 299, 00161 Rome, Italy

ARTICLE INFO

Article history:
Received 3 February 2017
Received in revised form
25 March 2017
Accepted 27 March 2017
Available online 29 March 2017

Keywords:
Giardia
NBDHEX
Thioredoxin reductase
Elongation factor 1Bγ

ABSTRACT

Giardiasis, a parasitic diarrheal disease caused by *Giardia duodenalis*, affects one billion people worldwide. Treatment relies only on a restricted armamentarium of drugs. The disease burden and the increase in treatment failure highlight the need for novel, safe and well characterized drug options. The antitumoral compound NBDHEX is effective *in vitro* against *Giardia* trophozoites and inhibits glycerol-3-phosphate dehydrogenase. Aim of this work was to search for additional NBDHEX protein targets. The intrinsic NBDHEX fluorescence was exploited in a proteomic analysis to select and detect modified proteins in drug treated *Giardia*. *In silico* structural analysis, intracellular localization and functional assays were further performed to evaluate drug effects on the identified targets. A small subset of *Giardia* proteins was covalently bound to the drug at specific cysteine residues. These proteins include metabolic enzymes, e.g. thioredoxin reductase (gTrxR), as well as elongation factor 1B-γ (gEF1Bγ), and structural proteins, e.g. α-tubulin. We showed that NBDHEX *in vitro* binds to recombinant gEF1Bγ and gTrxR, but only the last one could nitroreduce NBDHEX leading to drug modification of gTrxR catalytic cysteines, with concomitant disulphide reductase activity inhibition and NADPH oxidase activity upsurge. Our results indicate that NBDHEX reacts with multiple targets whose roles and/or functions are specifically hampered. In addition, NBDHEX is in turn converted to reactive intermediates extending its toxicity. The described NBDHEX pleiotropic action accounts for its antigiardial activity and encourages the use of this drug as a promising alternative for the future treatment of giardiasis.

1. Introduction

Giardiasis is an ubiquitous gastrointestinal disease caused by the flagellated protozoan parasite *Giardia duodenalis* (syn. *lamblia* or *intestinalis*) infecting the gut of mammals, including humans. Almost one billion people are estimated to be infected worldwide, including Europe, with a higher disease burden in developing countries (over 200 million symptomatic cases/year) (Lane and Lloyd, 2002). Infection occurs following ingestion of parasite cysts present either in contaminated water or food or via the fecal-oral route by host-to-host contact. Trophozoites, released from the cysts, multiply and colonize the upper part of the host small intestine, adhere to enterocyte surface and cause the symptoms, such as acute and chronic diarrheal disease. Infections may be also asymptomatic (Buret, 2008). Giardiasis is prevalent in children (other risk groups include returning travellers and immigrants/refugees) (Shah et al., 2009; Staat et al., 2011), with prolonged/recurrent infections correlated to failure to thrive syndrome in malnourished children. Post-infectious long term consequences of giardiasis, including post-infectious irritable bowel syndrome, have been also reported (Buret, 2008). Consequently, treatment of clinical giardiasis is recommended. Nitroimidazoles, whose prototype is metronidazole (MTZ), and other nitrocompounds, e.g. nitazoxanide, are the most used therapeutic agents (Lalle, 2010; Ansell et al., 2015). Benzimidazoles, including the anthelmintic

* Corresponding author.
** Corresponding author.
E-mail addresses: riccig@uniroma2.it (G. Ricci), marco.lalle@iss.it (M. Lalle).

http://dx.doi.org/10.1016/j.ijpddr.2017.03.006

albendazole, are also used with lower efficacy. Despite their therapeutic value, all these compounds provoke from mild to serious side effects. Treatment failures with MTZ have been reported in 10–20% of patients, especially returning travellers from poor endemic countries (Muñoz Gutiérrez et al., 2013; Yadav et al., 2014; Ansell et al., 2015). Therefore, an implementation of the available anti-giardial arsenal with more potent, safe and well tolerated drugs are desirable. Novel classes of compounds, some already approved for unrelated human diseases treatment, are effective against *Giardia* (Tejman-Yarden et al., 2013; Hahn et al., 2013; Kulakova et al., 2014) and potential drug targets have been also identified (Reyes-Vivas et al., 2014; Debnath et al., 2014; Galkin et al., 2014).

We have proven that the anticancer agent 6-(7-nitro-2,1,3-benzoxadiazol-4-ylthio)hexanol (NBDHEX) is five times more potent than MTZ in killing *Giardia* trophozoites (NBDHEX IC_{50}: 0.3 ± 0.1 μM; MTZ IC_{50}: 1.5 ± 0.1 μM) (Lalle et al., 2015). NBDHEX is a "mechanism-based inhibitor" of human glutathione-S-transferases (GSTs) promoting apoptosis in a variety of cancer cell lines with good tolerability and safety profile in mouse model (Ricci et al., 2005; Turella et al., 2005, 2006; Sau et al., 2012). Since neither GST and glutathione cycling nor canonical apoptotic pathways are present in *Giardia* (Bagchi et al., 2012; Ansell et al., 2015), our data indicate that reduction of NBDHEX nitro moiety in the parasite environment, associated with ROS generation, is likely involved in cytotoxicity (Lalle et al., 2015).

MTZ and other nitrocompounds (i.e. nitroimidazoles, nitrofurans and nitrothiazolides) are enzymatically nitroreduced to nitroradical anions, forming adducts with DNA, proteins and free thiols leading to DNA damage, protein inactivation and generating oxidative stress (Müller, 1983; Ansell et al., 2015). In *Giardia*, pyruvate ferredoxin oxidoreductase (PFOR) and its ferredoxin substrate, thioredoxin reductase (TrxR), nitroreductase1 (NR1) and the NADH oxidase, have been implicated in the activation of nitrodrugs (Ansell et al., 2015).

In *Giardia* trophozoites, NBDHEX administration induces a significant reduction of the FAD-dependent glycerol-3-phosphate dehydrogenase (gG3PD) activity (Lalle et al., 2015). *In vitro*, gG3PD is able to nitroreduce NBDHEX, but not MTZ, resulting in the formation of covalent adducts between nitroreduced NBDHEX and several enzyme cysteine residues. Additionally, spectroscopic analyses suggest that oxidized NBDHEX, which is intrinsically fluorescent, can bind gG3PD, likely via σ-complexes (Lalle et al., 2015). Since small molecule drugs can target multiple proteins in the same organisms, the identification of all possible binding partners is an essential step to fully understand the mechanism(s) of activity and advance the drug development process.

Taking advantage of the intrinsic NBDHEX fluorescence properties, we present a proteomic and functional analysis of NBDHEX-treated *Giardia* trophozoites aimed at detecting additional protein targets.

2. Materials and methods

2.1. Parasite cultivation and drug treatment

Giardia WB-C6 was used and cultivated as described (Lalle et al., 2015). Ethanol-dissolved NBDHEX (50 μM), synthetized as described (Ricci et al., 2005), or solvent alone, was added to confluent culture of *Giardia* trophozoites for 2 h at 37 °C (Lalle et al., 2015). Parasite soluble proteins were prepared as described (Lalle et al., 2015) from 2×10^9 trophozoites. Protein concentration was determined by Bradford methods (Thermo Fisher Scientific).

2.2. Vector construction, expression and purification of the recombinant proteins

The full-length coding sequences of gTrxR and gEF1Bγ (GiardiaDB accession number GL50803_9827 and GL50803_12102, respectively) were PCR amplified from the *Giardia* WB-C6 genomic DNA using primers reported in Supplemental Table S1. PCRs were performed on a T-Personal Thermocycler (Biometra, Göttingen, Germany) using 100 ng of gDNA, 10 units of high fidelity Pfu turbo DNA polymerase (Agilent Technologies, Santa Clara, CA, USA), 50 μM dNTP, 20 pmol of each primer in 50 μl of reaction mixture. Amplification conditions were: 1 cycle at 95 °C for 2 min; 30 cycles at 95 °C for 30 s, 56 °C for 30 s and 72 °C for 30 s; and 1 cycle at 72 °C for 7 min. The coding sequence of g14-3-3 was excised from p14-X vector3. For the expression of N-terminal 6xHIS-tagged fusion protein in *Escherichia coli*, the *Bam*HI/*Not*I digested fragments were cloned in *Bam*HI/*Not*I linearized pQ30 vector (Qiagen, Germany) and transformed in M15 strain. Expression of recombinant proteins and purification under native conditions by metal affinity chromatography (Qiagen, Germany) were performed as described (Lalle et al., 2015).

2.3. Production of polyclonal antibodies

BALB/c mice (Charles River Laboratories International, Inc., MA, USA) were intraperitoneally immunized with either purified HIS-gTrxR or HIS-gEF1Bγ. Fifty μg of protein were inoculated on day 0 in 300 μl of emulsified 1:1 PBS/Freund's complete adjuvant (Sigma Aldrich), on day 21 in 1:1 PBS/Freund's incomplete adjuvant (Sigma Aldrich) and without adjuvant on day 42. Blood samples were collected before initial immunization and after each boost from the tail vein. Sera fractions were assayed for specific antibody content.

2.4. Western blot analysis

Proteins were separated on a NuPAGE 4–12% (Novex, Invitrogen, Carlsbad, CA, USA) as described (Lalle et al., 2015). Antibodies used were: mouse polyclonal sera anti-gTrxR and anti-gEF1Bγ, 1:3000 (see Supplemental Information); mouse polyclonal (pAb) anti-gADI and anti-gOCT (Ringqvist et al., 2008), 1:2000; mouse monoclonal (mAb) anti-HA (Sigma-Aldrich), 1:3000; mouse anti-αTubulin (clone B-5-1-2, Sigma-Aldrich), 1:10000; mouse anti-HIS mAb (Qiagen), 1:2000. Interaction was revealed by incubation with HRP-cojugated secondary Ab (1:3000) followed by chemiluminescence (Millipore, France).

2.5. Confocal laser scanning microscopy (CLSM)

CLSM analyses of trophozoites were performed on a Leica TCS SP2 AOBS apparatus (Leica Microsystems, Germany) as described15. Antibodies used were: mouse polyclonal anti-gTrxR and anti-gEF1Bγ sera, 1:50; mouse anti-gADI and anti-gOCT4, 1:100; mouse anti-αTubulin mAb (clone B-5-1-2), 1:200; FITC-conjugated mouse anti-HA mAb (Miltenyi Biotec, Germany), 1:50; Alexa-Fluor 647- and 488-conjugated anti-rabbit and anti-mouse secondary Ab (Invitrogen), 1:500. Image deconvolution was performed with Huygens software (Scientific Volume Imaging BV, The Netherlands).

2.6. Enzymatic assay for gTrxR, spectrophotometric and fluorimetric analysis

HIS-gTrxR activity was assayed in continuous at 412 nm (25 °C) with Uvikon 941 Plus spectrophotometer (Kontron Instruments,

Watford, Herts, UK) in 1 ml standard assay mixture (4 mM DTNB, 50 μM NADPH in 0.1 M potassium phosphate buffer, pH 7.4) at different enzyme concentrations. TNB- release was calculated on the extinction coefficient of 14,200 M-1cm-1. The Km for DTNB was determined at fixed NADPH (50 μM) and variable DTNB concentrations (0.1–4 mM range) and the Km for NADPH was determined at fixed DTNB (4 mM) and variable NADPH concentrations (1.5–50 μM range) in 0.1 M potassium phosphate buffer, pH 7.4, at 25 °C. The NADPH oxidase activity was assayed in 1 ml of standard assay mixture, without disulfides, with HIS-gTrxR (10 μg) with 0.2 mM NADPH with increasing amount of NBDHEX. The Km for NADPH was evaluated using different NADPH concentrations (0.25–25 μM range). The UV–visible and the fluorescence (λex at 430 nm) spectra of NBDHEX (100 μM) were recorded overtime at 25 °C in a Multiskan Spectrum (Thermo) spectrophotometer and Luminescence Spectrometer LS50B (Perkin Elmer, Waltham, MA, USA), respectively.

2.7. NBDHEX inhibition of and binding to HIS-gTrxR

NBDHEX inhibition of thioreductase activity was assayed in 1 ml of standard assay mixture with HIS-gTrxR (0.44 μM) and increasing amount of drug (0.1–53 μM range). Biphasic inhibition pattern was analyzed using PRISM 6.0 software (GraphPad Software, Inc; La Jolla, CA, USA). Isothermal binding of NBDHEX to HIS-gTrxR was evaluated on the basis of intrinsic protein fluorescence quenching. Measurements were performed using 0.44 μM HIS-gTrxR with increasing NBDHEX amounts (0.1–53 μM range) in 0.1 M potassium phosphate buffer, pH 7.4, on a Fluoromax-4 spectrofluorometer (Horiba, UK) at 25 °C (λex at 295 and λem at 340 nm; slit width at 5.5 nm) and data corrected for inner filter effect.

NBDHEX binding to HIS-gEF1Bγ. NBDHEX binding to HIS-gEF1Bγ was evaluated according to intrinsic protein fluorescence quenching. Assay conditions were 0.38 μM HIS-gEF1Bγ with increasing NBDHEX amounts (0.12–4.5 μM range) in 0.01 M potassium phosphate buffer, pH 7.4. Excitation and emission wavelengths were 280 nm and 340 nm, respectively. Fluorescence spectra (λex at 432 nm) of 1.23 nmoles of NBDHEX at pH 7.4 were recorded by adding increasing amount of HIS-gEF1Bγ (0.5–2.7 nmoles range).

2.8. Mass spectrometry (MS) analysis

Proteins were separated on a 1D-gel NuPAGE 4–12% (Novex, Invitrogen) run in MOPS buffer and stained with the Colloidal Blue Staining kit (Invitrogen). Slices were excised and digested with trypsin (Promega Corporation, France), as previously described (Shevchenko et al., 1996). LC-MS/MS analyses of peptide mixtures were performed as described6. Entirely independent experiments were repeated in triplicate. Tandem mass spectra were matched against the *Giardia* protein database (GiardiaDB version 1.2) through the SEQUEST algorithm (Bioworks version 3.3, Thermo Electron). Precursor and fragment ions were searched with 1.5 and 1 Da tolerance, respectively. The following match parameters were taken into account: fully tryptic cleavage constraints (one miscleavage allowed); static cysteine carbamidomethylation and variable methionine oxidation. Putative NBDHEX adducts on cysteine or lysine residues were searched for by taking into account the formation of intact or partially or completely nitro-reduced NBDHEX adducts as well as addition of NBDHEX fragments only. Statistical parameters used to legitimate protein identification were as described (Lalle et al., 2012).

2.9. Bioinformatic analysis

Amino acid sequences of proteins analyzed in this work were downloaded from either GiardiaDB (http://giardiadb.org/giardiadb) or UniProt database (http://www.uniprot.org). Conserved functional domains and sites in the protein sequence were searched using ELM (http://elm.eu.org/) and BLASTp (https://blast.ncbi.nlm.nih.gov/Blast.cgi) algorithms. Multiple sequence analyses were performed with MultAlin tool (http://multalin.toulouse.inra.fr/multalin/multalin.html) and manually refined. Homology modelling was performed using SwissModel (https://swissmodel.expasy.org/). In the case of gEF1Bγ, which is a particularly difficult target, we also used model building programs that consistently provided reliable protein structure predictions in community-wide Critical Assessment of Structure Prediction (CASP) experiments, such as I-TASSER (http://zhanglab.ccmb.med.umich.edu/I-TASSER/), HHPred (https://toolkit.tuebingen.mpg.de/hhpred) and Phyre2 (http://www.sbg.bio.ic.ac.uk/phyre2/html/page.cgi?id=index). PsiPred Disopred3 program (http://bioinf.cs.ucl.ac.uk/psipred/) was used to predict gEF1Bγ disordered regions. The 3D structures of proteins homologous to gEF1Bγ analyzed in this work (see Supplemental Figs. S4 and S11) were downloaded from the Protein Data Bank (PDB, http://www.rcsb.org/pdb/home/home.do). SwissPDBViewer (http://spdbv.vital-it.ch/) and InsightII (Accelrys Inc.) were used for visualization and analyses of experimentally determined structures and 3D models. Following models to templates comparisons, the best model provided by I-TASSER for gEF1Bγ N-terminal (GST-like) and C-terminal (EF1Bγ-like) domains were chosen for further studies. Optimal structure alignments shown in Supplemental Figs. S4 and S11 were obtained by manually refining the initial automatic superposition provided by SwissPDBViewer to include the highest possible number of residues whose Ca-Ca distance was below 3 Å. The model of gEF1Bγ N-terminal GST-like domain (residues 1–197) in complex with NBDHEX was built by transferring NBDHEX coordinates from the 3D structure of the complex with human π-class GSTP1-1, determined by X-ray crystallography (PDB ID: 3gus, Resolution: 1.53 Å) after optimal model to structure superposition, and performing small manual adjustments to relieve unfavourable van der Waals contacts. Electrostatic potential was calculated using the APBS program (http://www.poissonboltzmann.org/) and mapped on the solvent accessible surface of the protein model using PyMol.

3. Results

3.1. Identification of NBDHEX targets in Giardia trophozoites

We exploited the intrinsic NBDHEX fluorescence properties to identify new protein targets in *Giardia*. NBDHEX treated trophozoites resulted faintly fluorescent under UV light, confirming the intracellular drug accumulation (Lalle et al., 2015). Indeed, following SDS-PAGE, several protein bands were UV light fluorescent only in NBDHEX-treated samples (Fig. 1A). Fluorescent bands were analyzed by LC-MS/MS looking for the presence of cysteines or lysines modified by intact (NBDHEX-NO_2), partially (NBDHEX-NHOH) or completely (NDHEX-NH_2) nitro-reduced NBDHEX. We identified proteins (Table 1) with peptides carrying one or more cysteines with a 265 Da mass increment compatible with NBDHEX-NH_2 adducts (Fig. 1B and C and Supplemental Fig. S1). Despite the fluorescence associated with the protein bands could be ascribable to unreduced NBD moiety, no peptide modified with NBDHEX-NO_2, NBDHEX-NHOH or NBD alone was identified. No modified peptide belonging to gG3PD (Lalle et al., 2015) was detected, likely due to the low protein abundance.

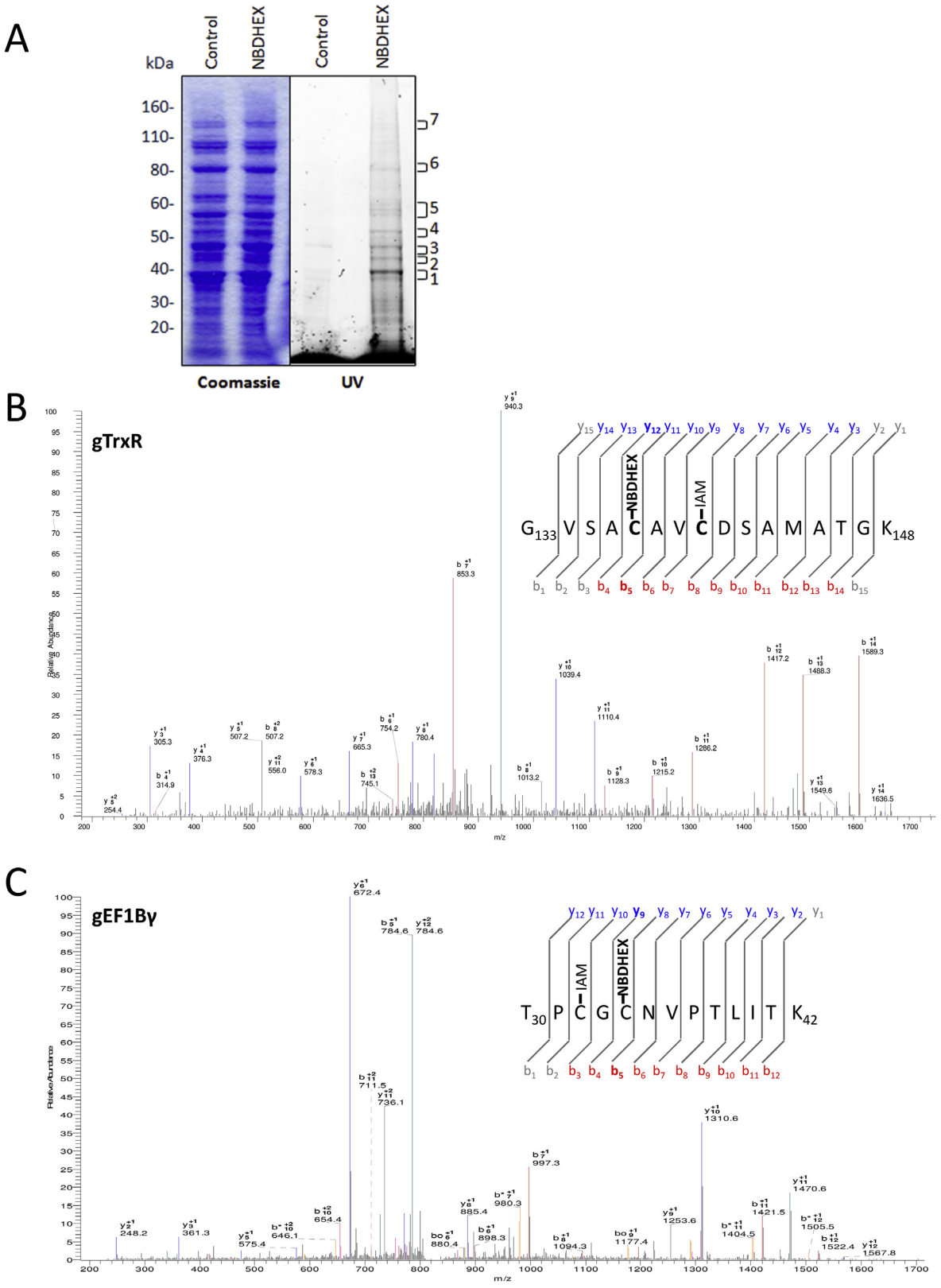

Fig. 1. Proteomic identification of NBDHEX targets. A) Representative SDS-PAGE of soluble proteins (50 μg) from *Giardia* trophozoites treated or not with NBDHEX under UV light (right) and after Coomassie staining (left). Molecular size markers are indicated on the left. B) and C) Representative MS/MS spectra of gTrxR peptide 133–148 (B) and gEF1Bγ peptide 30–42 (C) acquired after trypsin digestion of fluorescent bands 1 and 6. NBDHEX indicates cysteines (Cys137 in gTrxR and Cys34 in gEF1Bγ) with mass increase of 265 Da and IAM indicates iodoacetamide-alkylated cysteines.

Table 1
Giardia proteins with NBDHEX adducts identified by MS/MS in UV-fluorescent bands after SDS-PAGE.

Protein name	MW (kDa)	GiardiaDB accession no (UniProt)	Adduct position	No of experiments
Thioredoxin Reductase (gTrxR)	33.8	GL50803_9827 (E2RU27)	C_{137} and/or C_{140}	3
Ornithine Cabamoyl Transferase (gOCT)	36.4	GL50803_10311 (E2RTT6)	C_{16}	3
Elongation Factor 1Bγ (gEF1Bγ)	45.2	GL50803_12102 (A8BFR0)	C_{32} and/or C_{34}	3
α-Tubulin (gα-TUB)	50.5	GL50803_103676 (A8BPC0)	C_{347}	1
Arginine deiminase (gADI)	64.1	GL50803_112103 (E2RU36)	C_{283}	1
Pyruvate flavodoxin oxidoreductase (gPFOR-2)	131.7	GL50803_17063 (A8B852)	C_{967}	1
Axoneme-associated protein GASP-180 (gGASP-180)	174.5	GL50803_137716 (A8B5G1)	C_{889}	1

3.2. Structural and/or functional roles of NBDHEX modified cysteines

Only one or two cysteines were found to be specifically NBDHEX-modified in each protein. To infer the mechanism of selective cysteine targeting and the biological consequences of such modifications, structural/functional role of these cysteines was investigated.

The NADPH-dependent flavoenzyme gTrxR belongs to the 35 KDa low molecular weight group, having the redox-active disulfide CXXC in the active site (Hirt et al., 2002). In the absence of the GSH system in *Giardia,* gTrxR plays a major role in redox homeostasis and antioxidant defence (Brown et al., 1996; Ansell et al., 2015). Both NBDHEX-modified Cys137 and Cys140 correspond to the redox-active cysteines as inferred by multiple sequence alignment and homology model built for gTrxR (Supplemental Fig. S2).

Both gADI and gOCT participate in the arginine dihydrolase metabolism for energy production and defence towards the host environment (Schofield et al., 1992; Stadelmann et al., 2013). According to gADI homology model (Trejo-Soto et al., 2016), the drug modified Cys283 is proximal to the catalytic His280 and to arginine substrate stabilizing residue Arg282. In the homo-trimeric structure of gOCT (Galkin et al., 2009) the drug-modified Cys16 sits far away from the catalytic site, in a region exposed to the solvent (Supplemental Fig. S3).

The gEF1Bγ is a structural component of the eukaryotic elongation factor 1 (eEF1) complex, which catalyzes the aminoacyl-tRNA delivery step (Sasikumar et al., 2012). The gEF1Bγ comprises an N-terminal and C-terminal domain, belonging to the GST and EF1γ families, respectively, connected by a disordered region (~30 residues) (Koonin et al., 1994; Jeppesen et al., 2003). GST activity has been proved for human, rice and *Aspergillus* EF1Bγ (Kobayashi et al., 2001; Carberry et al., 2006; Achilonu et al., 2014). Homology models were built for each of the two domains separately, since no experimentally determined structure comprising both domains was available (Supplemental Fig. S4). Cys32 and Cys34 reside in the N-terminal GST-like domain at the rim of the cavity formed by the N-terminal and C-terminal GST sub-domains and are fully solvent accessible (Supplemental Fig. S4, panel c).

The modified Cys347 of gα-TUB can be located at the interface between α- and β-tubulin oligomer (Supplemental Fig. S5), suggesting NBDHEX adduct may interfere with tubulin oligomerization.

In fermentative glycolysis of anaerobic organisms, gPFOR catalyzes the oxidative decarboxylation of pyruvate, with reduction of ferredoxin (Horner et al., 1999). Two PFOR isoforms are encoded by *Giardia*. The gPFOR-1 is also involved in metronidazole nitroreduction (Leitsch et al., 2011). We identified gPFOR-2 among NBDHEX targets, with the modified Cys967, absent in gPFOR-1, located in a loop of the domain VI' (Chabrière et al., 1999), far from the thiamine pyrophosphate cofactor binding site and from the three putative [4Fe-4S] clusters (Chabrière et al., 1999) (Supplemental Fig. S6).

The information available on gGASP-180, a member of an unusual *Giardia* cytoskeletal protein family (Elmendorf et al., 2005), was too limited to argue about the significance of Cys899-NBDHEX adduct.

3.3. NBDHEX affects physical properties and intracellular localization of target proteins

Nitroimidazole adducts formation has been shown to induce molecular size and isoelectric point shift of *Giardia* proteins (Leitsch et al., 2012). Indeed, following *Giardia* exposure to NBDHEX, gOCT and gTrxR shifted towards higher molecular sizes, with the latter showing a band doublet, as observed in immunoblot experiments (Fig. 2A). For both gEF1By and gα-TUB, a faint extra band appeared at lower molecular size, due either to partial degradation or altered mobility of protein-adduct. Moreover, bands compatible with dimeric and tetrameric gEF1Bγ were almost visible in the drug-treated sample, suggesting that NBDHEX may promote gEF1Bγ oligomerization. No effect could be seen on gADI or on g14-3-3, the latter used as negative control (Fig. 2A). Exploiting NBDHEX autofluorescence (Lalle et al., 2015), we performed co-localization experiments by CLSM. NBDHEX fluorescence was mainly associated to perinuclear area, median body and intracellular flagellar roots (Fig. 2B). Localization of gADI (panels c and f), gEF1Bγ (panels l to n) or α-gTUB (panels b and e) was apparently unaffected. Nevertheless, NBDHEX and α-gTUB signals co-localized (pseudocolor yellow) particularly at the median body (Fig. 2B, panel e). Following NBDHEX treatment, gOCT stained as puncta in the cytosol with partial re-localization/accumulation in the perinuclear region, co-localizing with NBDHEX (Fig. 2b panels a, d). In untreated parasites, gTrxR stained strongly and homogenously the cytoplasm, being present also in nuclei (Fig. 2B, panel g). After drug treatment (Fig. 2B, panels h and i), gTrxR staining was less intense in the nuclei but increased in the perinuclear area, co-localizing with NBDHEX. Although cytosolic staining persisted, areas devoid of the gTrxR could be visible in ~15% of parasites.

3.4. Effect of NBDHEX on HIS-tagged gTrxR and gEF1By expressed in E. coli

Since gTrxR and gEF1Bγ have been recognized as MTZ activator

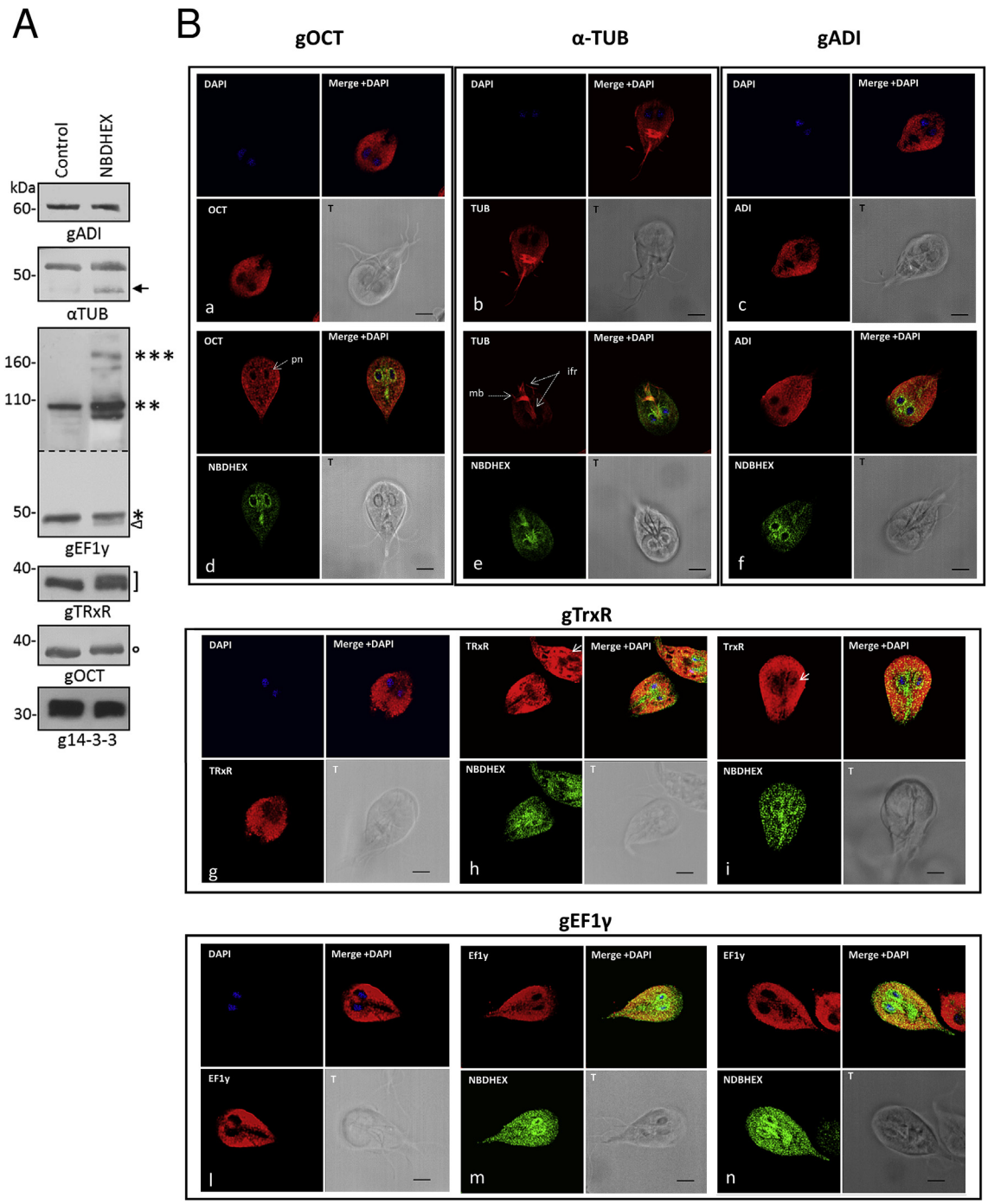

Fig. 2. NBDHEX effect on target protein electrophoretic mobility and intracellular localization. A) Representative Western blot analysis of soluble proteins from *Giardia* trophozoites incubated or not with NBDHEX. The low molecular weight bands of α-gTUB (arrow) and gEF1Bγ (triangle) are indicated. Asterisks indicate the molecular size corresponding to monomeric (*), dimeric (**) and multimeric (***) gEF1Bγ. The circle indicates the gOCT band shifted at higher molecular size. The square bracket indicates a gTrxR bands pair. The panel corresponding to the Western blot with anti-gEF1Bγ is a combination of two exposure times B) CLSM analysis of *Giardia* trophozoites incubated with (panels d, e, f, h, i, m and n) or without (panels a, b, c, g and l) NBDHEX. NBDHEX (green) was directly visualized using the laser light at λem 488 nm. Parasites were stained with the indicated mouse antibodies and anti-mouse AlexaFluor 647-conjugated (red). Nuclei were stained with DAPI (blue). Pn: perinuclear area; mb: median body; ifr: intracellular flagellar roots. Displayed micrographs correspond to a single z-stack. T, transmission light acquisition. Scale bar 5 μm. (For interpretation of the references to colour in this figure legend, the reader is referred to the web version of this article.)

and/or drug targets, respectively (Leitsch et al., 2012), their interplay with NBDHEX was further studied using bacterial expressed HIS-tagged recombinant proteins. After drug treatment of *E. coli*, purified HIS-gTrxR and HIS-gEF1Bγ showed fluorescence after SDS-PAGE (Fig. 3), supporting the formation of stable NBDHEX-protein complexes. As in drug treated trophozoites (Fig. 2A), a lower band was associated to purified HIS-gEF1Bγ from NBDHEX-treated bacteria. No effect on HIS-gEF1Bγ oligomerization was noticed (Fig. 3B). As in *Giardia*, MS analysis (Supplemental Fig. S7) confirmed the same cysteine-NBDHEX adducts in the purified proteins.

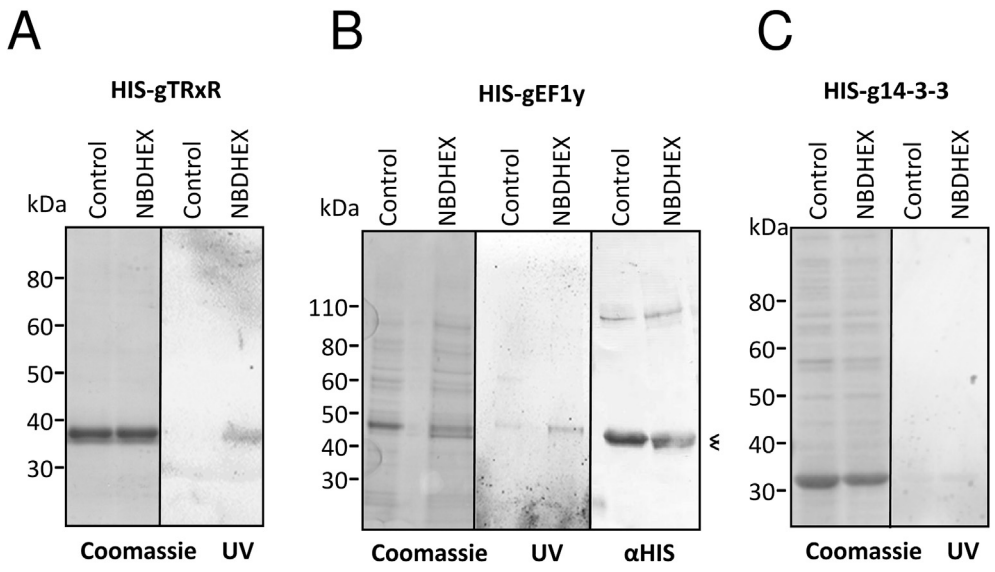

Fig. 3. NBDHEX binds to recombinant His-tagged gTrxR and HIS-gEF1Bγ expressed in bacteria. Recombinant proteins, expressed in *E. coli* and affinity purified after treatment of bacteria with NBDHEX (50 μM) or ethanol for 2 h, were separated on 4–12% PAGE, visualized on UV-transilluminator (UV), stained with Coomassie or blotted and probed with mAb anti-HIS (αHIS). The double bands of gEF1Bγ are indicated by the "less than" symbol (<).

3.5. In vitro NBDHEX binds to gTrxR, inhibits its activity towards disulfides and enhances its NADPH oxidase activity

Drug binding to purified HIS-gTrxR was characterized by protein intrinsic fluorescence quenching. Even in the absence of NADPH, NBDHEX binds to HIS-gTrxR with high affinity with a two phase binding behaviour, K_{d1} = 0.14 ± 0.05 μM, ending to 50% of the overall quenching, and K_{d2} = 13 ± 1 μM (Fig. 4A). The effect of NBDHEX on disulphide reductase activity was assessed using DTNB as generic TrxR substrate (Brown et al., 1996; Leitsch et al., 2011). Neither thioredoxin nor other physiological substrates of gTrxR has been yet identified (Leitsch et al., 2011). Using NADPH as co-substrate, HIS-gTrxR reduces DTNB with k_{cat} = 4.8 ± 0.3 s^{-1} (DTNB K_m = 1.5 ± 0.1 mM and NADPH K_m = 2.6 ± 0.6 μM) (Supplemental Fig. S8). NBDHEX strongly inhibited the reaction (Fig. 4B) with a biphasic trend and K_i values (K_{i1} = 0.15 ± 0.05 μM and K_{i2} = 14 ± 1 μM) very similar to the measured K_d. Kinetic analysis (data not shown) indicated that NBDHEX is competitive inhibitor of DTNB, suggesting a partial overlapping of two compounds binding sites. In the absence of disulfide substrates and under aerobic conditions, *Entamoeba histolytica* TrxR displays NADPH oxidase activity (Arias et al., 2012) and oxygen reduction activity was shown for gTrxR (Leitsch et al., 2012). Indeed, HIS-gTrxR oxidizes NADPH with (K_m = 0.5 ± 0.1 μM) (data not shown). In presence of NBDHEX, NADPH oxidase activity increased up to five fold (Fig. 5A), with hemi-activation at NBDHEX 14 μM (Fig. 5B), indicating that oxidase activity mainly occurs at the expense of NBDHEX fully saturated enzyme (Fig. 5B). During this catalytic process, HIS-gTrxR also modifies NBDHEX as indicated by absorption spectrum shift from 432 nm to ~455 nm (Fig. 5C), loss of the fluorescence emission peak at 525 nm, and yellow to orange colour shift (Fig. 5D). As also observed for gG3PD (Lalle et al., 2015), such modifications are compatible with gTrxR-mediated drug nitroreduction. We asked if Cys137 and Cys140 adducts could result from gTrxR activity toward NBDHEX. While incubation of HIS-gTrxR with NADPH alone resulted in electrophoretic mobility increased in SDS-PAGE (Fig. 5E), incubation with NBDHEX alone not only increased HIS-gTrxR mobility but made also protein band fluorescent, evidence of a SDS-resistant drug-protein complex (Fig. 5E). Co-incubation with NADPH and NBDHEX decreased both

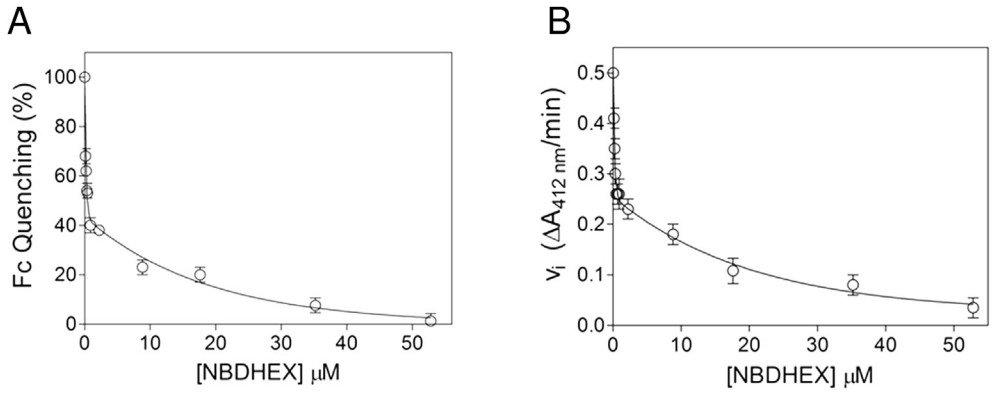

Fig. 4. NBDHEX binding to and inhibitory effect on HIS-gTrxR A) Analysis of HIS-gTrxR intrinsic fluorescence quenching after incubation was reacted with different amounts of NBDHEX. Experimental points were fitted to a bi-phasic binding curve. B) Inhibition of HIS-gTrxR thioreductase activity by NBDHEX. DTNB thioreductase activity was followed at 412 nm where the enzymatic product (TNB^-) absorbs. Inhibition data were obtained incubating HIS-gTrxR, NADPH and DTNB with increasing amounts of NBDHEX as detailed in Methods.

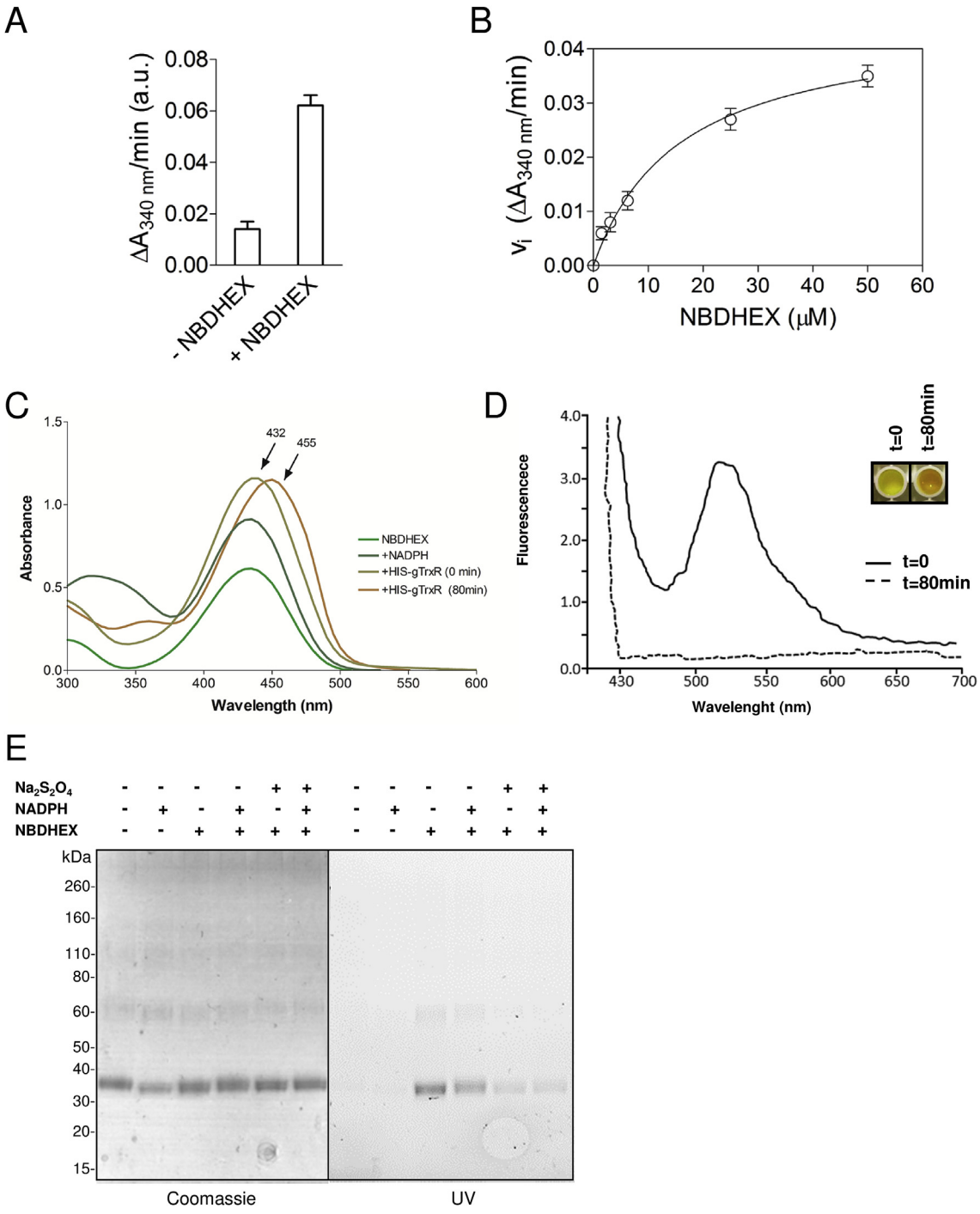

Fig. 5. Effect of NBDHEX on NADPH oxidase activity of gTrxR and NADPH-dependent gTrxR activity on NBDHEX. A) Oxidation of NADPH by gTrxR in presence or absence of saturating NBDHEX (60 μM). B) NBDHEX-dependent oxidation of NADPH by gTrxR at pH 7.4. Emiactivation is at 16 μM. C) UV–visible spectrum of NBDHEX recorded either in the presence of NADPH alone (dark green line) after the addition of HIS-gTrxR at t = 0 (mustard line) or after 80 min of incubation (orange line). Maximal absorption wavelength (nm) is indicated (arrow). D) Fluorescence spectra of NBDHEX (excitation at 430 nm) incubated with HIS-gTrxR at t = 0 (solid line) or after 80 min (dashed line) in the presence of NADPH. The change in color of the reaction is shown in the insert. E) SDS-PAGE of HIS-gTrxR after 80 min incubation with or without NBDHEX, in the presence or not of NADPH. Subsequent treatment of the reaction mixture with sodium dithionite ($Na_2S_2O_4$) is also indicated. Gel was photographed under UV light (UV, right panel) before staining with Coomassie blue (Coomassie, left panel). (For interpretation of the references to colour in this figure legend, the reader is referred to the web version of this article.)

HIS-gTrxR-associated fluorescence and mobility (Fig. 5E), consistent with enzyme-mediated reduction of the nitro moiety of at least a fraction of bound NBDHEX. This is supported by the remarkable decrease of HIS-gTrxR-associated fluorescence occurring after the addition of the nitroreducing agent $Na_2S_2O_4$ (Lalle et al., 2015). Finally, NBDHEX modified cysteines were the same as those reported in Table 1 (Supplemental Fig. S9). However, band associated fluorescence suggested the presence of HIS-gTrxR subset tightly bound to unreduced/partially reduced NDBHEX, although not detectable in our MS experiments.

3.6. HIS-tagged gEF1Bγ forms a complex with but does not reduce NBDHEX

A distinctive brown colour (data not shown) and UV–visible spectrum of HIS-gEF1Bγ, showing two absorbance peaks with one centred at ~415 nm (Fig. 6A), are suggestive of protein bound iron likely as iron-sulfur cluster (Crack et al., 2004). HIS-gEF1Bγ-NBDHEX interaction was monitored studying intrinsic protein fluorescence quenching. High affinity binding of NBDHEX to HIS-gEF1Bγ (K_d < 0.4 μM) showed a monophasic behaviour (Fig. 6B). No modification of NBDHEX absorption spectrum was observed even at equimolar amounts of HIS-gEF1Bγ (data not shown). Conversely, NBDHEX fluorescence spectrum showed a slight increase and a 530 nm–520 nm blue-shift (Fig. 6C) and, since NBD fluorescence is sensitive to environmental polarity (Frey and Tamm, 1990), this suggested drug entering into a protein hydrophobic pocket. As well, the formation of cysteine adducts with the sole NBD moiety, still fluorescent, cannot be excluded since they could be masked by HIS-gEF1Bγ absorbance in the same wavelength range (415–420 nm) (Ellis and Poole, 1997). Intriguingly and in agreement with the NBDHEX-induced gEF1Bγ oligomerization (Fig. 2A), NBDHEX binding to HIS-gEF1Bγ promotes a fast protein aggregates not fractionable by classical chromatographic procedures (data not shown).

In non-reducing SDS-PAGE, HIS-gEF1By associated fluorescence increased as consequence of NBDHEX incubation (Fig. 6D) while decreased after $Na_2S_2O_4$ treatment. Nevertheless, modified peptides displayed a 132 Da mass increase (Supplemental Fig. S10) compatible with the formation of a disulfide bond between cysteines and the thiohexanolic group of NBDHEX, as confirmed by disappearance of these adducts after DTT treatment. In cell free condition, our observations support the formation of a stable complex between the HIS-gEF1Bγ and oxidized NBDHEX, whilst not detected by mass spectrometry. Conversely, *in cell* treatment, the identification of gEF1Bγ cysteine adducts with the nitroreduced drug is ascribable to nitroreductases present in the cell environment (e.g. gTrxR).

To rationalize the molecular basis of NBDHEX/gEF1Bγ interaction, the protein 3D model was further processed to locate NBDHEX binding site. In solved GST-NBDHEX complex structures (i.e., PDB: 3gus and 3gur), the drug binds to residues comprised within the GST cavity and involved in GSH binding, most of which are located within structurally conserved regions (Supplemental Fig. S11, panel a, b). The gEF1Bγ modelled NBDHEX binding site appears to be only moderately polar (Supplemental Fig. S11, panel c), in agreement with a decrease in the polarity of NBDHEX environment upon interaction with the protein, as suggested by the drug fluorescence shift (Fig. 6C). These observations support NBDHEX binding to gEF1Bγ N-terminal GST-like domain in a similar orientation to that observed in the homologous structures. In the model of gEF1Bγ N-terminal GST-like domain in complex with NBDHEX, the location of the latter is compatible with formation of a disulfide bond between Cys34 and the thiohexanolic portion of the drug.

4. Discussion

In the present work we have both identified additional NBDHEX targets and proposed new mechanisms underlying its cytotoxicity in *Giardia* trophozoites. Although aminic forms of NBD derivatives are not fluorescent (McIntyre and Sleight, 1991; Ellis and Poole, 1997), the drug targets were isolated within fluorescent bands but only specific cysteine-NBDHEX-NH_2 adducts were detected. σ-Complexes between NBDHEX and sulphur nucleophiles (Federici et al., 2009) as well as adducts between NBD-Cl and protein cysteines (Bragg and Hou, 1999) easily form and are fluorescent, but they have never been detected by MS. As for nitroimidazoles (e.g.,

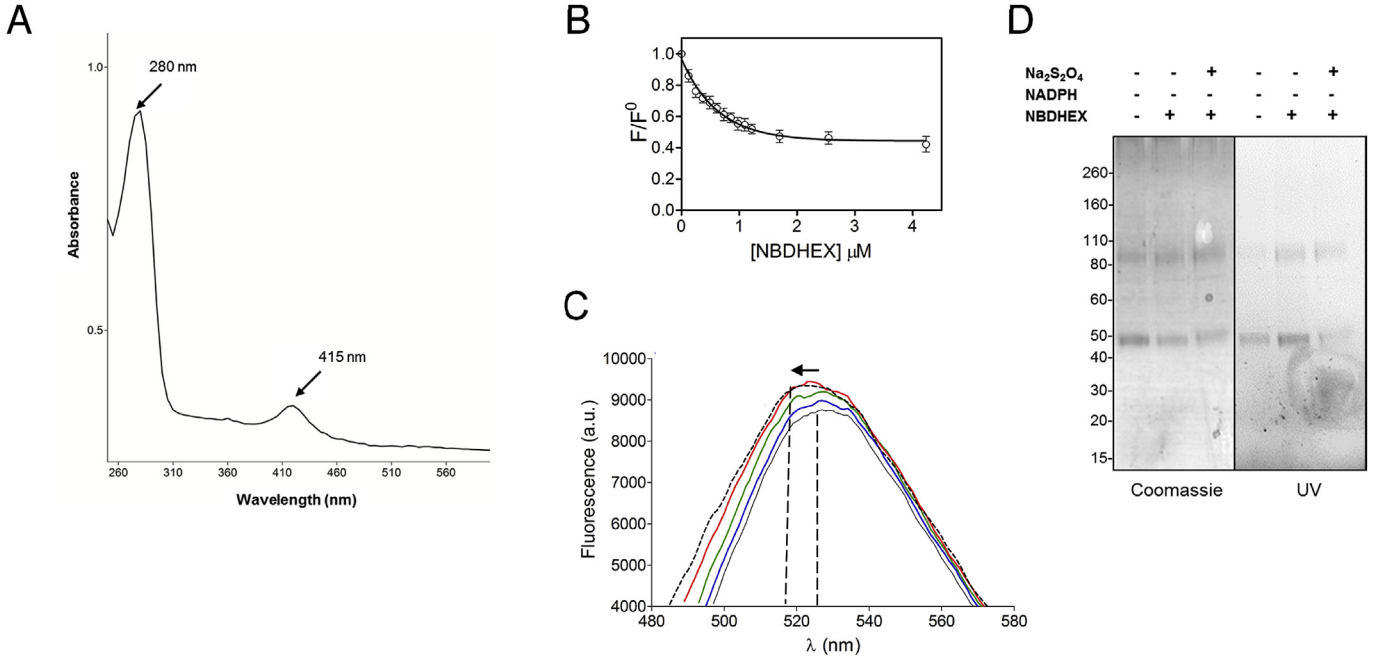

Fig. 6. NBDHEX binding to gEF1By. A) UV–visible spectrum of HIS-gEF1Bγ recorded at 25 °C. Peak maxima are reported. Spectrum is representative of three independent experiments. B) Binding of NBDHEX to HIS-EF1Bγ. Quenching of intrinsic HIS-EF1Bγ fluorescence caused by NBDHEX binding was monitored at 340 nm (excitation at 280 nm). C) Changes in NBDHEX fluorescence emission spectra due to HIS-EF1Bγ binding. NBDHEX in the absence of HIS-gEF1Bγ (gray line) and in the presence of increasing HIS-gEF1Bγ amounts: blue, green, red and dashed line. Excitation wavelength was at 432 nm. Vertical lines indicate ~530 and ~520 nm, while the arrow indicates the "blue-shift" of NBDHEX fluorescence. D) SDS-PAGE of HIS-EF1Bγ after 80 min incubation with or without NBDHEX. Subsequent treatment of the reaction mixture with sodium dithionite ($Na_2S_2O_4$) is also indicated. Gel was photographed under UV light (UV, right panel) before staining with Coomassie blue (Coomassie, left panel). (For interpretation of the references to colour in this figure legend, the reader is referred to the web version of this article.)

MTZ) (Müller, 1983; Kedderis et al., 1989; Ansell et al., 2015), NBDHEX may undergo biochemical reduction to radical anion and further react with cysteine residues (Supplemental Fig. S12). Cysteine adducts with reduced NBDHEX-NHOH have been previously detected for gG3PD (Lalle et al., 2015), albeit for none of the herein identified targets.

We clearly demonstrate that NBDHEX exerts an inhibitory effect on gTrxR covalently binding its catalytic cysteines. Also nitroimidazoles and auranofin target and inhibit gTrxR, but their inhibition mechanism is still unknown (Leitsch et al., 2012, 2016). The observed biphasic binding and inhibitory effect of NBDHEX on gTrxR thioreductase activity associate to the TrxRs homodimeric character. Drug binding can occur with higher affinity to the first and with lower affinity to the second catalytic site, or a not yet detected site beyond the catalytic one may account for low affinity binding.

We observed that NBDHEX is a competitive inhibitor of DTNB reduction. In the gTrxR flavin oxidized conformation, electrons are transferred from FAD to the active disulphide (Hirt et al., 2002) with a significant rotation of NADPH-binding domain respect to the FAD binding domain (Hirt et al., 2002). In the flavin reduced conformation, NADPH reduces FAD while the catalytic cysteines reduce the substrate. In this conformation, NBDHEX and DTNB binding sites overlap, in agreement with the competitive inhibition observed. *In vivo*, NBDHEX binding to gTrxR catalytic cysteines can prevent electron transfer to the downstream thiol substrate(s), interfering with parasite redox homeostasis, and increases gTrxR NADPH oxidase activity accounting for even more dramatic effects.

As well, NBD-Cl promotes *in vitro* NADPH oxidase activity of other flavoproteins reacting with their active site dithiol and being concomitantly reduced (Carlberg and Mannervik, 1980). Other TrxRs display an ancillary NADPH oxidase activity (Arias et al., 2012) but its biological significance is still unclear. Indeed, it futilely consumes NADPH, impairing cofactor-dependent processes, and can generate ROS in presence of O_2. Dissolved O_2 (dO_2) concentration fluctuates from 0 to 80 μM in the host intestine where *Giardia* resides (Espey, 2013). The gTrxR NADPH oxidase activity could increase *Giardia* susceptibility to O_2. This seems in contrast with the observation that overexpression of either TrxR or TrxR disulphide reductase null mutant leads to an increment of TrxR-associated NADPH oxidase activity, as measured in parasite extract, but does not hamper parasite duplication time under standard growth conditions (Leitsch et al., 2016). However, the NAD(P)H:menadione oxidoreductase over-expression was associates with *Giardia* susceptibility to O_2 only when parasite was grown under aerobic condition, when oxygen is used instead of menadione and superoxide anion and H_2O_2 are overproduced (Li and Wang, 2006).

More important as generator redox stress is that 6-(7-nitro-2,1,3-benzoxadiazol-4-ylthio) derivatives can undergo, in the presence of oxygen and before complete nitroreduction of NBD-moiety, several redox-cycles thus efficiently consuming O_2 and dramatically generating ROS (Patridge et al., 2012). Simultaneously, the generated intermediates possess electrophilic scavenging activity and can react with cellular components.

In vivo reduction of NBDHEX by gTrxR could be also independent from dO_2 concentration. Sarcoplasmic reticulum NADH-dependent oxidases reduce NBD-Cl at similar rates under aerobic or low O_2 concentration by species other than superoxide ions, such as short-chain sugars (Olojo et al., 2005). All the proposed mechanisms could contribute to gTrxR-mediated NBDHEX toxicity.

Upon drug administration to trophozoites, gEF1Bγ is covalently modified at Cys32 and/or Cys34 by NBDHEX. gEF1Bγ forms uncharacterized covalent adducts with MTZ and tinidazole, whereas ronidazole induces gEF1Bγ degradation (Leitsch et al., 2012). No enzymatic activity or function has been associated with gEF1Bγ, not even the structural role demonstrated in eEF complex. Although no functional relevance can be inferred for Cys32 and Cys34, this CXC motif is unique for EF1Bγ from *Giardia* and *Spironucleus salmonicida*. CXC resides in a loop exposed to solvent within a region, structurally equivalent to the GSH binding site of GSTs and with a thioredoxin-like folding[52]. Indeed, natural mutations of catalytic CXXC motif to CXCC of *E. coli* TrxA led to the formation of dimeric TrxA bridged by a [2Fe-2S] iron-sulfur cluster coordinated by the first and the second cysteines from each subunit (Collet et al., 2005). These mutations reverse the conventional TrxA function, so that the protein promotes disulfide bonds formation instead of reduction (Collet et al., 2005). Dimerization of gEF1Bγ by [2Fe-2S] iron-sulfur cluster coordination is likely to occur, at least when expressed in bacteria, but a similar behaviour and gEF1Bγ involvement in disulfide bonds formation are to be proven in *Giardia*. It has been proposed that GST domain of eukaryotic EF1Bγ mediates EF1 complex assembly by disulfide bond exchange between endogenous GSSG and protein in the complex (Koonin et al., 1994). Similarly, gEF1Bγ could exploit this function via a Trx-like and GSH independent mechanism. Although EF1Bγs are already dimeric, NBDHEX can block one the cysteines of gEF1Bγ CXC motif likely and promotes the formation of intermolecular disulfide bound, mediating the observed highly stable oligomers and interfering with gEF1Bγ associated processes. Indeed, Cys to Ser mutation of one of *B. subtilis* TrxA catalytic cysteines results in the formation of mixed disulfide intermediate between TrxA and substrates or another TrxA molecule (Kouwen et al., 2008). These single-cysteine mutants display oxidation of the remaining active-site cysteine residue, resulting in homodimerization by disulfide bound formation (Kouwen et al., 2008).

gADI and gOCT perform central functions in *Giardia* and their targeting by NBDHEX may contribute to deregulate arginine metabolism. NBD derivatives display core structural similarity with the benzimidazoles. *In silico* prediction suggests that benzimidazole nucleus can form hydrophobic interactions or hydrogen bonds with residues in gADI catalytic site (Trejo-Soto et al., 2016), including NBDHEX-modified Cys283. This supports NBDHEX binding to gADI catalytic cavity. Ultimately NBDHEX nitroradicals can covalently modify Cys283. Impact on protein gADI function need to be ascertained.

NBDHEX modification of gOCT Cys16 could instead be a result of a physical interaction of gOCT with other proteins, being Cys16 far from the catalytic site but in a region exposed to the solvent. Indeed, gOCT has been co-precipitated with GlNR2, a nitroreductase known to reduce MTZ and nitazoxanide (Müller et al., 2015). Similarly, GASP-180 interacts with the other *Giardia* nitroreductase GlNR1, also active toward several nitrocompounds (Müller et al., 2015). The direct involvement of GlNR1 and GlNR2 on NBDHEX nitroreduction to form intermediates reactive with gOCT and gGASP-180 could be taken into account.

NBDHEX and benzimidazoles core structural similarities contribute to understant α-tubulin targeting by NBDHEX. The benzimidazole-2-carbamate derivatives, albendazole and nocodazole, inhibit microtubule polymerization binding to β-tubulin monomer of several parasites, including *Giardia* (MacDonald et al., 2004). Homology modelling and molecular docking locate albendazole binding site in the region involved in heterodimerization with α-tubulin (Aguayo-Ortiz et al., 2013). NBDHEX-modified α-tubulin Cys347 locates to the other site of the heterodimerization domain therefore it does not face β-tubulin albendazole binding site. In polymerized microtubules (Supplemental Fig. S5), Cys347 would locate at the interface between two α-β heterodimers, in a region encompassing the binding domain of vinca alkaloids, another class of microtubule-destabilizing agents (Gigant et al.,

2005). Even though direct evidence need to be provided, we can speculate that impairing of microtubule polymerization/dynamics could be among the cytotoxic effects exerted by NBDHEX.

Among the proposed cytotoxic effects exerted by NBDHEX, we may not exclude a further imbalance of redox equilibrium due to a drug-mediated decrease of the intracellular non-protein thiol pool, as already reported for other nitrocompounds (Leitsch et al., 2012). Moreover, DAPI stained DNA in nuclei of trophozoites exposed to NBDHEX were strongly condensed (data not shown), suggesting a direct effect of the drug on the DNA, in agreement with MTZ being a DNA damaging agent (Uzlikova and Nohynkova, 2014). However these two aspects need still to be addressed.

In conclusion, the NBDHEX pleiotropic action makes this compound a good candidate drug as alternative anti-*Giardia* treatment and deserves to be further investigated also in animal model of giardiasis.

Acknowledgments

We are grateful to Dr. Donatella Pietraforte, Istituto Superiore di Sanità, Italy, for the fruitful discussion. We also acknowledge Prof. Staffan Svard, Uppsala University, for the gift of anti-gADI and anti-gOCT antibodies. This research did not receive any specific grant from funding agencies in the public, commercial, or not-for-profit sectors.

Appendix A. Supplementary data

Supplementary data related to this article can be found at http://dx.doi.org/10.1016/j.ijpddr.2017.03.006.

References

Achilonu, I., Siganunu, T.P., Dirr, H.W., 2014. Purification and characterisation of recombinant human eukaryotic elongation factor 1 gamma. Protein Expr. Purif. 99, 70–77.

Aguayo-Ortiz, R., Méndez-Lucio, O., Romo-Mancillas, A., Castillo, R., Yépez-Mulia, L., Medina-Franco, J.L., Hernández-Campos, A., 2013. Molecular basis for benzimidazole resistance from a novel β-tubulin binding site model. J. Mol. Graph. Model 45, 26–37.

Ansell, B.R., McConville, M.J., Ma'ayeh, S.Y., Dagley, M.J., Gasser, R.B., Svärd, S.G., Jex, A.R., 2015. Drug resistance in *Giardia duodenalis*. Biotechnol. Adv. 33, 888–901.

Arias, D.G., Regner, E.L., Iglesias, A.A., Guerrero, S.A., 2012. *Entamoeba histolytica* thioredoxin reductase: molecular and functional characterization of its atypical properties. Biochim. Biophys. Acta 1820, 1859–1866.

Bagchi, S., Oniku, A.E., Topping, K., Mamhoud, Z.N., Paget, T.A., 2012. Programmed cell death in *Giardia*. Parasitology 139, 894–903.

Bragg, P.D., Hou, C., 1999. Effect of NBD chloride (4-chloro-7-nitrobenzo-2-oxa-1,3-diazole) on the pyridine nucleotide transhydrogenase of *Escherichia coli*. Biochim. Biophys. Acta 1413, 159–171.

Brown, D.M., Upcroft, J.A., Upcroft, P., 1996. A thioredoxin reductase-class of disulphide reductase in the protozoan parasite *Giardia duodenalis*. Mol. Biochem. Parasitol. 83, 211–220.

Buret, A.G., 2008. Pathophysiology of enteric infections with *Giardia duodenalis*. Parasite 15, 261–265.

Carberry, S., Neville, C.M., Kavanagh, K.A., Doyle, S., 2006. Analysis of major intracellular proteins of Aspergillus fumigatus by MALDI mass spectrometry: identification and characterization of an elongation factor 1B protein with glutathione transferase activity. Biochem. Biophys. Res. Commun. 341, 1096–1104.

Carlberg, I., Mannervik, B., 1980. Interaction of 2,4,6-trinitrobenzenesulfonate and 4-chloro-7-nitrobenzo-2-oxa-1,3-diazole with active sites of glutathione reductase and lipoamide dehydrogenase. Acta Chem. Scand. B 34 (2), 144–146.

Chabrière, E., Charon, M.H., Volbeda, A., Pieulle, L., Hatchikian, E.C., Fontecilla-Camps, J.C., 1999. Crystal structures of the key anaerobic enzyme pyruvate: ferredoxin oxidoreductase, free and in complex with pyruvate. Nat. Struct. Biol. 6, 182–190.

Collet, J.F., Peisach, D., Bardwell, J.C., Xu, Z., 2005. The crystal structure of TrxA(-CACA): insights into the formation of a [2Fe-2S] iron-sulfur cluster in an *Escherichia coli* thioredoxin mutant. Protein Sci. 14, 1863–1869.

Crack, J., Green, J., Thomson, A.J., 2004. Mechanism of oxygen sensing by the bacterial transcription factor fumarate-nitrate reduction (FNR). J. Biol. Chem. 279, 9278–9286.

Debnath, A., Shahinas, D., Bryant, C., Hirata, K., Miyamoto, Y., Hwang, G., Gut, J., Renslo, A.R., Pillai, D.R., Eckmann, L., Reed, S.L., McKerrow, J.H., 2014. Hsp90 inhibitors as new leads to target parasitic diarrheal diseases. Antimicrob. Agents Chemother. 58, 4138–4144.

Ellis, H.R., Poole, L.B., 1997. Novel application of 7-chloro-4-nitrobenzo-2-oxa-1,3-diazole to identify cysteine sulfenic acid in the AhpC component of alkyl hydroperoxide reductase. Biochemistry 36, 15013–15018.

Elmendorf, H.G., Rohrer, S.C., Khoury, R.S., Bouttenot, R.E., Nash, T.E., 2005. Examination of a novel head-stalk protein family in *Giardia lamblia* characterised by the pairing of ankyrin repeats and coiled-coil domains. Int. J. Parasitol. 35, 1001–1011.

Espey, M.G., 2013. Role of oxygen gradients in shaping redox relationships between the human intestine and its microbiota. Free Radic. Biol. Med. 55, 130–140.

Federici, L., Lo Sterzo, C., Pezzola, S., Di Matteo, A., Scaloni, F., Federici, G., Caccuri, A.M., 2009. Structural basis for the binding of the anticancer compound 6-(7-nitro-2,1,3-benzoxadiazol-4-ylthio)hexanol to human glutathione s-transferases. Cancer Res. 69, 8025–8034.

Frey, S., Tamm, L.K., 1990. Membrane insertion and lateral diffusion of fluorescence-labelled cytochrome c oxidase subunit IV signal peptide in charged and uncharged phospholipid bilayers. Biochem. J. 272, 713–719.

Galkin, A., Kulakova, L., Wu, R., Gong, M., Dunaway-Mariano, D., Herzberg, O., 2009. X-ray structure and kinetic properties of ornithine transcarbamoylase from the human parasite *Giardia lamblia*. Proteins 76, 1049–1053.

Galkin, A., Kulakova, L., Lim, K., Chen, C.Z., Zheng, W., Turko, I.V., Herzberg, O., 2014. Structural basis for inactivation of *Giardia lamblia* carbamate kinase by disulfiram. J. Biol. Chem. 289, 10502–10509.

Gigant, B., Wang, C., Ravelli, R.B., Roussi, F., Steinmetz, M.O., Curmi, P.A., Sobel, A., Knossow, M., 2005. Structural basis for the regulation of tubulin by vinblastine. Nature 435, 519–522.

Hahn, J., Seeber, F., Kolodziej, H., Ignatius, R., Laue, M., Aebischer, T., Klotz, C., 2013. High sensitivity of *Giardia duodenalis* to tetrahydrolipstatin (orlistat) in vitro. PLoS One 8 pii=e71597.

Hirt, R.P., Müller, S., Embley, T.M., Coombs, G.H., 2002. The diversity and evolution of thioredoxin reductase: new perspectives. Trends Parasitol. 18, 302–308.

Horner, D.S., Hirt, R.P., Embley, T.M., 1999. A single eubacterial origin of eukaryotic pyruvate: ferredoxin oxidoreductase genes: implications for the evolution of anaerobic eukaryotes. Mol. Biol. Evol. 16, 1280–1291.

Jeppesen, M.G., Ortiz, P., Shepard, W., Kinzy, T.G., Nyborg, J., Andersen, G.R., 2003. The crystal structure of the glutathione S-transferase-like domain of elongation factor 1Bgamma from Saccharomyces cerevisiae. J. Biol. Chem. 278, 47190–47198.

Kedderis, G.L., Argenbright, L.S., Miwa, G.T., 1989. Covalent interaction of 5-nitroimidazoles with DNA and protein in vitro: mechanism of reductive activation. Chem. Res. Toxicol. 2, 146–149.

Kobayashi, S., Kidou, S., Ejiri, S., 2001. Detection and characterization of glutathione S-transferase activity in rice EF-1betabeta'gamma and EF-1gamma expressed in *Escherichia coli*. Biochem. Biophys. Res. Commun. 288, 509–514.

Koonin, E.V., Mushegian, A.R., Tatusov, R.L., Altschul, S.F., Bryant, S.H., Bork, P., Valencia, A., 1994. Eukaryotic translation elongation factor 1 gamma contains a glutathione transferase domain–study of a diverse, ancient protein superfamily using motif search and structural modeling. Protein Sci. 3, 2045–2054.

Kouwen, T.R., Andréll, J., Schrijver, R., Dubois, J.Y., Maher, M.J., Iwata, S., Carpenter, E.P., van Dijl, J.M., 2008. Thioredoxin A active-site mutants form mixed disulfide dimers that resemble enzyme-substrate reaction intermediates. J. Mol. Biol. 379, 520–534.

Kulakova, L., Galkin, A., Chen, C.Z., Southall, N., Marugan, J.J., Zheng, W., Herzberg, 3, 2014. Discovery of novel antigiardiasis drug candidates. Antimicrob. Agents Chemother. 58, 7303–7311.

Lalle, M., Camerini, S., Cecchetti, S., Sayadi, A., Crescenzi, M., Pozio, E., 2012. Interaction network of the 14-3-3 protein in the ancient protozoan parasite *Giardia duodenalis*. J. Proteome Res. 11, 2666–2683.

Lalle, M., Camerini, S., Cecchetti, S., Finelli, R., Sferra, G., Müller, J., Ricci, G., Pozio, E., 2015. The FAD-dependent glycerol-3-phosphate dehydrogenase of *Giardia duodenalis*: an unconventional enzyme that interacts with the g14-3-3 and it is a target of the antitumoral compound NBDHEX. Front. Microbiol. 6, 544.

Lalle, M., 2010. Giardiasis in the post genomic era: treatment, drug resistance and novel therapeutic perspectives. Infect. Disord. Drug. Targets 10, 283–294.

Lane, S., Lloyd, D., 2002. Current trends in research into the waterborne parasite *Giardia*. Crit. Rev. Microbiol. 28, 123–147.

Leitsch, D., Burgess, A.G., Dunn, L.A., Krauer, K.G., Tan, K., Duchêne, M., Upcroft, P., Eckmann, L., Upcroft, J.A., 2011. Pyruvate:ferredoxin oxidoreductase and thioredoxin reductase are involved in 5-nitroimidazole activation while flavin metabolism is linked to 5-nitroimidazole resistance in *Giardia lamblia*. J. Antimicrob. Chemother. 66, 1756–1765.

Leitsch, D., Müller, J., Müller, N., 2016. Evaluation of *Giardia lamblia* thioredoxin reductase as drug activating enzyme and as drug target. Int. J. Parasitol. Drugs. Drug. Resist 6, 148–153.

Leitsch, D., Schlosser, S., Burgess, A., Duchêne, M., 2012. Nitroimidazole drugs vary in their mode of action in the human parasite *Giardia lamblia*. Int. J. Parasitol. Drugs Drug. Resist 2, 166–170.

Li, L., Wang, C.C., 2006. A likely molecular basis of the susceptibility of Giardia lamblia towards oxygen. Mol. Microbiol. 59, 202–211.

MacDonald, L.M., Armson, A., Thompson, A.R., Reynoldson, J.A., 2004. Characterisation of benzimidazole binding with recombinant tubulin from *Giardia duodenalis*, *Encephalitozoon intestinalis*, and *Cryptosporidium parvum*. Mol. Biochem. Parasitol. 138, 89–96.

McIntyre, J.C., Sleight, R.G., 1991. Fluorescence assay for phospholipid membrane asymmetry. Biochemistry 30, 11819–11827.
Müller, J., Rout, S., Leitsch, D., Vaithilingam, J., Hehl, A., Müller, N., 2015. Comparative characterisation of two nitroreductases from *Giardia lamblia* as potential activators of nitro compounds. Int. J. Parasitol. Drugs Drug. Resist 5, 37–43.
Müller, M., 1983. Mode of action of metronidazole on anaerobic bacteria and protozoa. Surgery 93, 165–171.
Muñoz Gutiérrez, J., Aldasoro, E., Requena, A., Comin, A.M., Pinazo, M.J., Bardají, A., Oliveira, I., Valls, M.E., Gascon, J., 2013. Refractory giardiasis in Spanish travellers. Travel. Med. Infect. Dis. 11, 126–129.
Olojo, R.O., Xia, R.H., Abramson, J.J., 2005. Spectrophotometric and fluorometric assay of superoxide ion using 4-chloro-7-nitrobenzo-2-oxa-1,3-diazole. Anal. Biochem. 339, 338–344.
Patridge, E.V., Eriksson, E.S., Penketh, P.G., Baumann, R.P., Zhu, R., Shyam, K., Eriksson, L.A., Sartorelli, A.C., 2012. 7-Nitro-4-(phenylthio)benzofurazan is a potent generator of superoxide and hydrogen peroxide. Arch. Toxicol. 86, 1613–1625.
Reyes-Vivas, H., de la Mora-de la Mora, I., Castillo-Villanueva, A., Yépez-Mulia, L., Hernández-Alcántara, G., Figueroa-Salazar, R., García-Torres, I., Gómez-Manzo, S., Méndez, S.T., Vanoye-Carlo, A., Marcial-Quino, J., Torres-Arroyo, A., Oria-Hernández, J., Gutiérrez-Castrellón, P., Enríquez-Flores, S., López-Velázquez, G., 2014. Giardial triosephosphate isomerase as possible target of the cytotoxic effect of omeprazole in *Giardia lamblia*. Antimicrob. Agents Chemother. 58, 7072–7082.
Ricci, G., DeMaria, F., Antonini, G., Turella, P., Bullo, A., Stella, L., Filomeni, G., Federici, G., Caccuri, A.M., 2005. 7-Nitro-2,1,3-benzoxadiazoledervatives, a new class of suicide inhibitors for glutathione S-transferases. Mechanism of action of potential anticancer drugs. J. Biol. Chem. 280, 26397–16405.
Ringqvist, E., Palm, J.E., Skarin, H., Hehl, A.B., Weiland, M., Davids, B.J., Reiner, D.S., Griffiths, W.J., Eckmann, L., Gillin, F.D., Svärd, S.G., 2008. Release of metabolic enzymes by *Giardia* in response to interaction with intestinal epithelial cells. Mol. Biochem. Parasitol. 159, 85–91.
Sasikumar, A.N., Perez, W.B., Kinzy, T.G., 2012. The many roles of the eukaryotic elongation factor 1 complex. Wiley Interdiscip. Rev. RNA 3, 543–555.
Sau, A., Filomeni, G., Pezzola, S., D'Aguanno, S., Tregno, F.P., Urbani, A., Serra, M., Pasello, M., Picci, P., Federici, G., Caccuri, A.M., 2012. Targeting GSTP1-1 induces JNK activation and leads to apoptosis in cisplatin-sensitive and -resistant human osteosarcoma cell lines. Mol. Biosyst. 8, 994–1006.
Schofield, P.J., Edwards, M.R., Matthews, J., Wilson, J.R., 1992. The pathway of arginine catabolism in *Giardia intestinalis*. Mol. Biochem. Parasitol. 51, 29–36.
Shah, N., DuPont, H.L., Ramsey, D.J., 2009. Global etiology of travelers' diarrhea: systematic review from 1973 to the present. Am. J. Trop. Med. Hyg. 80, 609–614.
Shevchenko, A., Wilm, M., Vorm, O., Mann, M., 1996. Mass spectrometric sequencing of proteins silver-stained polyacrylamide gels. Anal. Chem. 68, 850–858.
Staat, M.A., Rice, M., Donauer, S., Mukkada, S., Holloway, M., Cassedy, A., Kelley, J., Salisbury, S., 2011. Intestinal parasite screening in internationally adopted children: importance of multiple stool specimens. Pediatrics 128, e613.
Stadelmann, B., Hanevik, K., Andersson, M.K., Bruserud, O., Svärd, S.G., 2013. The role of arginine and arginine-metabolizing enzymes during *Giardia* - host cell interactions in vitro. BMC Microbiol. 13, 256.
Tejman-Yarden, N., Miyamoto, Y., Leitsch, D., Santini, J., Debnath, A., Gut, J., McKerrow, J.H., Reed, S.L., Eckmann, L., 2013. A reprofiled drug, auranofin, is effective against metronidazole-resistant *Giardia lamblia*. Antimicrob. Agents Chemother. 57, 2029–2035.
Trejo-Soto, P.J., Aguayo-Ortiz, R., Yépez-Mulia, L., Hernández-Campos, A., Medina-Franco, J.L., Castillo, R., 2016. Insights into the structure and inhibition of *Giardia intestinalis* arginine deiminase: homology modeling, docking, and molecular dynamics studies. J. Biomol. Struct. Dy 34, 732–748.
Turella, P., Cerella, C., Filomeni, G., Bullo, A., De Maria, F., Ghibelli, L., Ciriolo, M.R., Cianfriglia, M., Mattei, M., Federici, G., Ricci, G., Caccuri, A.M., 2005. Proapoptotic activity of new glutathione S-transferase inhibitors. Cancer. Res. 65, 3751–3761.
Turella, P., Filomeni, G., Dupuis, M.L., Ciriolo, M.R., Molinari, A., De Maria, F., Tombesi, M., Cianfriglia, M., Federici, G., Ricci, G., Caccuri, A.M., 2006. A strong glutathione S-transferase inhibitor overcomes the P-glycoprotein-mediated resistance in tumor cells. 6-(7-Nitro-2,1,3-benzoxadiazol-4-ylthio)hexanol (NBDHEX) triggers a caspase-dependent apoptosis in MDR1-expressing leukemia cells. J. Biol. Chem. 281, 23725–23732.
Uzlikova, M., Nohynkova, E., 2014. The effect of metronidazole on the cell cycle and DNA in metronidazole-susceptible and -resistant Giardia cell lines. Mol. Biochem. Parasitol. 198, 75–81.
Yadav, P., Tak, V., Mirdha, B.R., Makharia, G.K., 2014. Refractory giardiasis: a molecular appraisal from a tertiary care centre in India. Indian J. Med. Microbiol. 32, 378–382.